Source: **Motorola**
Title: **Polarization Modeling, Path Statistics & Urban Canyon Model**
Document for: **Discussion**

1. SUMMARY

Polarization Modeling: Handsets and small devices do not have adequate space for a 2 to 4 element linear array. For this reason polarized antennas are likely to be the only practical implementation. This contribution presents a more complete step by step procedure describing how to generate a polarized model which is compatible to the current ray-based model.

Randomizing Power Delay Profiles and Azimuth Spreads: Monotonically decreasing power with delay or with angle represent the average channel behavior, but this is not characteristic of a given mobile drop. Thus in order to examine the sensitivity of using such an average behavior, a noise model was suggested in [1] and modified in [2] to produce randomized PDP and PAS characteristics which match measured profiles. Further details are given about this model with suggested values for randomizing the path powers.

Micro-cell parameter assumptions: A proposed micro-cell model was given in [3]. There are a number of questions about parameter settings, and implementation issues that need some further details. A number of questions are given.

Urban Canyon: Based on an analysis of recent measurements[4], a model for Angle of Arrival is given for the Urban Canyon scenario. A method for use is also presented.

2. DUAL-POLARIZATION SPATIAL CHANNEL MODEL

2.1 Algorithm

An analysis of polarization was given in [5] which is excerpted in Appendix A. This analysis provides a means to transmit in a given polarization, add the effect of de-polarization which is produced by the channel by means of the branch power ratio, and converting the de-polarized signal into a receive antenna at a new polarization.

A number of parameters are assumed to be the same for each polarization. These include: Azimuth Spread, Delay Spread, and each of the six rays.

In order to generate a polarized channel model, the following steps are used. Steps 1-12 represent the current channel generation algorithm. Steps 13-18 are additional steps to account for the polarized effects of the channel.

- **Step 1:** Choose a single channel scenario common to all drops (i.e. to be applied to the entire simulation).

- **Step 2:** Generate Drops. Assign geometry (LOS direction and distance of UE from NodeB), UE antenna structure orientation, UE speed vector direction and magnitude.

- **Step 3:** Select lognormal random draws for DS, AS (at NodeB: σ_{ASk}), LN as described in Section 3.4.2 below.

- **Step 4:** Assign N = 6 paths (for macro channels). Assign 6 random delays. Delays are ordered and the minimum delay is subtracted from all so that the first delay is always zero. k is the drop and UE index. Ratio values r are r=1.17 suburban macro, r=1.41 urban macro. Realization of random delays are made according to the model below:

$$\tau_n = -r_{DS}\sigma_{DSk}\log z_n \qquad z_n : U(0,1)$$

- **Step 5:** Assign a power to each path n

$$P_n = e^{\frac{(1-r_{DS})\cdot\tau_n}{r_{DS}\cdot\sigma_{DSk}}}\cdot 10^{-\xi_n} \quad \text{where} \quad \xi_n : N(0,\sigma^2{}_{RND})$$

where σ_{RND} is a shadowing randomization effect on the per-path powers. Value is TBD. Powers are normalized so that total power (for all six paths is equal to one).

- **Step 6:** Generation of AODs per path and ordering at NodeB. Random draws of AODs from $N(0, r^2{}_{AOD,CS}\cdot\sigma^2{}_{ASk})$. The $r_{AOD,CS}$ =1.07 (0.3 in dB) (Suburban macro), $r_{AOD,CS}$ =1.3 (1.0 in dB) (urban macro).

- **Step 7:** The 6 AODs generated in Step 6 are ordered in increasing absolute value and each of the six delays (Step 4) is assigned to each AOD. Increasing delays are matched to increasing relative AOD angle δ_n is defined in [6] based on their absolute value and deterministically.

- **Step 8:** 20 sub-rays are used to generate a 2^o Laplacian spread for each path (ray) at the NodeB. All 20 sub-rays have identical powers (1/20 of the path power) but random phase. Sub-components have a predefined fixed angle distribution as shown in [6].

- **Step 9:** At the UE, assign per-path (ray) AOA variance as a function of the path (ray) relative power. Draw the relative AOA (with respect to LOS) from a distribution: $N(0,\sigma^2{}_{AOA})$. Where 0 = LOS, and σ_{AoA} = 104.12(1-exp(-0.2175*|P_r|), with P_r equal to the fraction of power in the given path in dBr.

- **Step 10:** 20 sub-rays are used to generate a 35^o Laplacian spread for each path (ray) at the UE. All 20 sub-rays have identical powers (1/20 of the path power) but random phase. Sub-components have a predefined fixed angle distribution as shown in the [6].

- **Step 11:** Pairing of each NodeB sub-ray with a corresponding UE sub-ray is made to create the actual channel gain. Random pairing is used.

- **Step 12:** Assign antenna gains to NodeB paths (rays). Assign the antenna gain to each UE sub-ray.

- **Step 13:** For each of the 6 paths of step 4, generate 20 sub-rays to represent the portion of each signal that leaks into the quadrature antenna orientation due to scattering. Pair each of the new sub-rays with a corresponding sub-ray that was generated in step 8.

- **Step 14:**. Set the AOD and AOA of each sub-ray in step 13 equal to that of the corresponding sub-ray of the inline antenna orientation. (Orthogonal sub-rays arrive/depart at common angles.)

- **Step 15:** Set the phase angle of each sub-ray in step 13 to a random angle drawn from U(0,2pi).

- **Step 16:** The amplitude of each sub-ray in the quadrature orientation is set relative to the amplitude of each sub-ray in the inline orientation according to P2 = P1 - A - B*N(0,1), where A=0.34*(mean ray imbalance)+7.2 dB, and B=5.5dB is the standard deviation of the imbalance variation.

- **Step 17:** Decompose each of the inline and quadrature sub-rays into vertical and horizontal components based on the in-line and quadrature orientations.

- **Step 18:** At the receive antennas, decompose each of the vertical and horizontal components into components that are in-line and quadrature with the receive antennas and sum the in-line components.

The elevation spread will be defined as a separate parameter and would be used in defining the sub-ray spacings at the Node-B and UE.

The fading behavior between the cross pol elements will be a function of the per-ray spreads and the Doppler. The fading can be correlated with common component phases between orthogonal sub-rays.

3. RANDOMIZING POWER DELAY PROFILES

Figure 1 illustrates the effect observed in the evaluation of the Power Delay Profile. In order to produce the expected exponential characteristic of the average PDP with the constraint of the delays being distributed with an exponential, the powers must be weighted as described in Step 5 above. When the value of "r" is low, this causes the path powers to be limited. From observations of actual measured data, the values of "r" are sensitive to thresholds, and other measurement effects. Recent results[7] indicate that the r-value should be larger. The value of 2.2 appears to be a reasonable value, being close to the median value in [7]. This value is shown in Figure 1 to be also close to the exponential distribution which has been observed in measurements when the 6 powers are normalized to unity power. This normalization process removes the λ parameter making the exponential non-parametric.

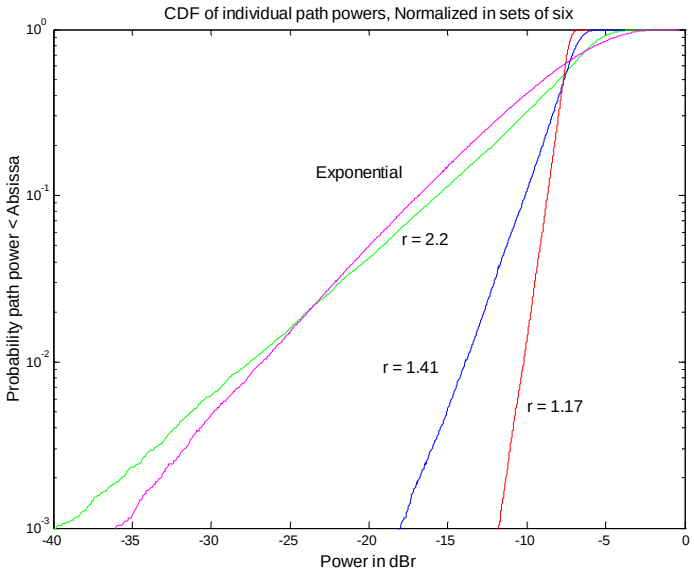

Figure 1 Power Distribution versus "r" value

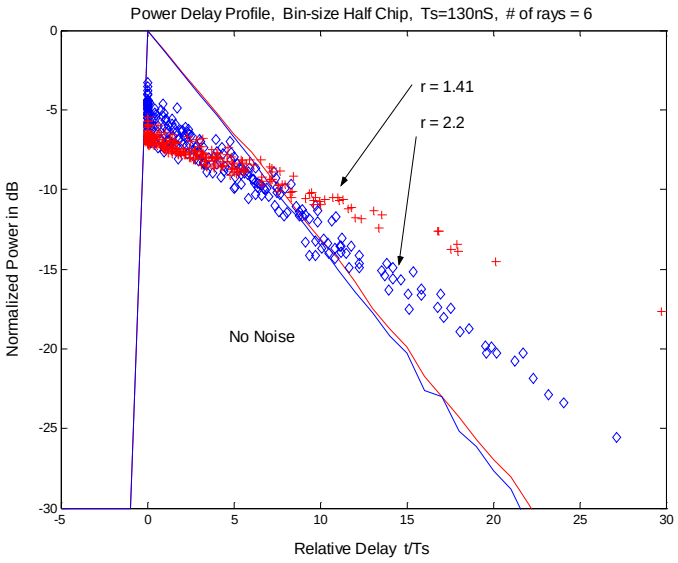

Figure 2 Power Delay Profile for two values of "r"

Figure 2 describes the PDP generated by the current model. The powers are monotonically decreasing with delay for each group of 6 path powers. Note that because they are normalized to unity power, there is some variation between the powers at each delay.

The powers of the rays observed in PDP measurements are not usually monotonically decreasing with time. In order to model the randomized behavior that is observed, a random noise model is suggested. This model appears in step 5 of the procedure above, which states:

$$P_n = e^{\frac{(1-r_{DS})\cdot\tau_n}{r_{DS}\cdot\sigma_{DSk}}} \cdot 10^{-\xi_n} \quad \text{where} \quad \xi_n : N(0,\sigma^2{}_{RND})$$

where σ_{RND} is a shadowing randomization effect on the per-path powers. Powers are normalized so that total power (for all six paths is equal to one).

From analyzing a number of Power Delay Profiles, and including the plot shown in [8] of the statistics of the PDP, a value of σ_{RND} = 4dB was chosen as a representative value. This value seems to produce a similar spread of values for each time delay. The result of the added noise is seen in Figure 3, which illustrates the dynamic range of powers that fall in the first time bin. Without the noise model, the powers were almost identical and the dynamic range was usually less than 1dB. With the noise model added, the median value of the difference between components that fall into the same time bin is 5dB. This model is suggested as a sensitivity test to determine the effect of realistic channels on a given technique.

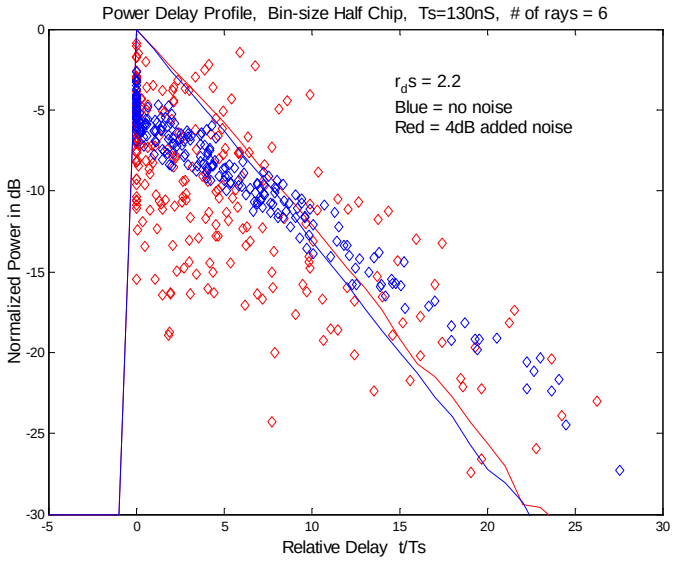

Figure 3 Example of PDP with and without Randomization

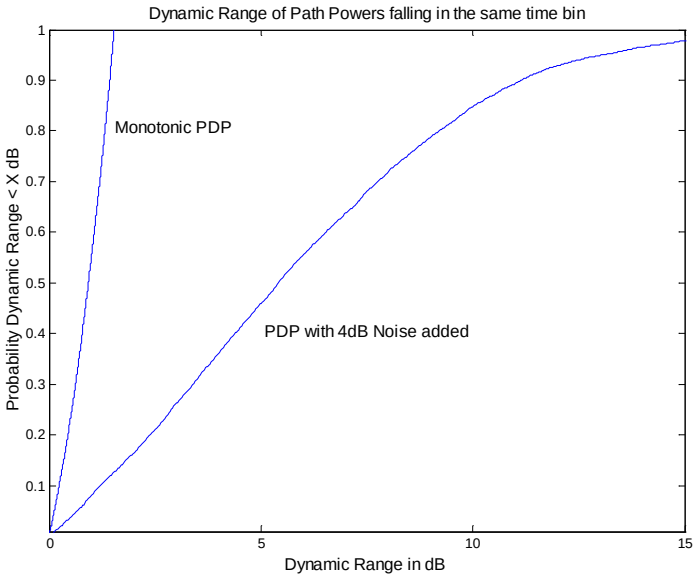

Figure 4 Dynamic Range of Path Powers falling the same time-bin

4. MICRO-CELL MODEL AND PARAMETER ASSUMPTIONS

A micro-cell model was proposed in [3]. The description of the model is very limited, and a number of questions remain to enable the model to be implemented.

The following list of parameters need further clarification:

1. Is the assumption to be strictly below rooftop?
2. What type of antenna patterns are assumed due to the cluttered effect of the micro-cell?
3. A new path-loss slope is needed to represent below rooftop cases.
4. Log Normal is proposed to be incorporated into the path components. How are these correlated to Log Normals for paths to near-by micro-cells?
5. What is the fraction of LOS paths that are in the coverage area of the micro-cell? Is this related to the Log Normal or Path Loss Model?
6. How will the fading model be modified in portions of the cell that are LOS, or on the same street as the micro-cell? E.g. Rician, K-factor?
7. Are Hexagonal repeats assumed for the layout of micro-cells? Is this assumed independent of the building grid?
8. Below rooftop micro-cells are typically dominated by urban canyon effects producing very distinct propagation behaviors. How will these be considered?

9. Delay spreads chosen from U(0, 800ns) seem to be constrained to a specific environment. Is this reasonable for a building grid environment?

10. The layout of the system can be drawn using different layout assumptions: hexagonal, or building grid, see Figure 5. These layout assumptions will have very different performance due to the directional nature of the environment.

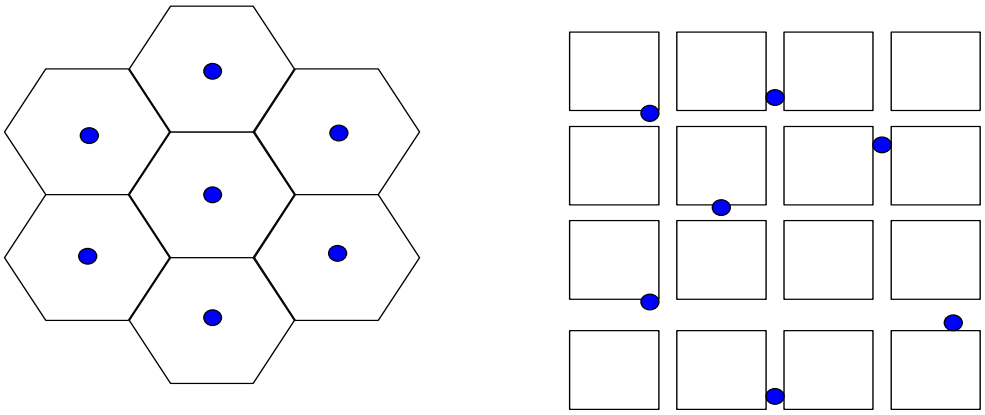

Figure 5 Two Different Micro-cell Geometries

5. URBAN CANYON MODEL

The following represents measured data extracted from [4], and evaluated to obtain the AoA probability.

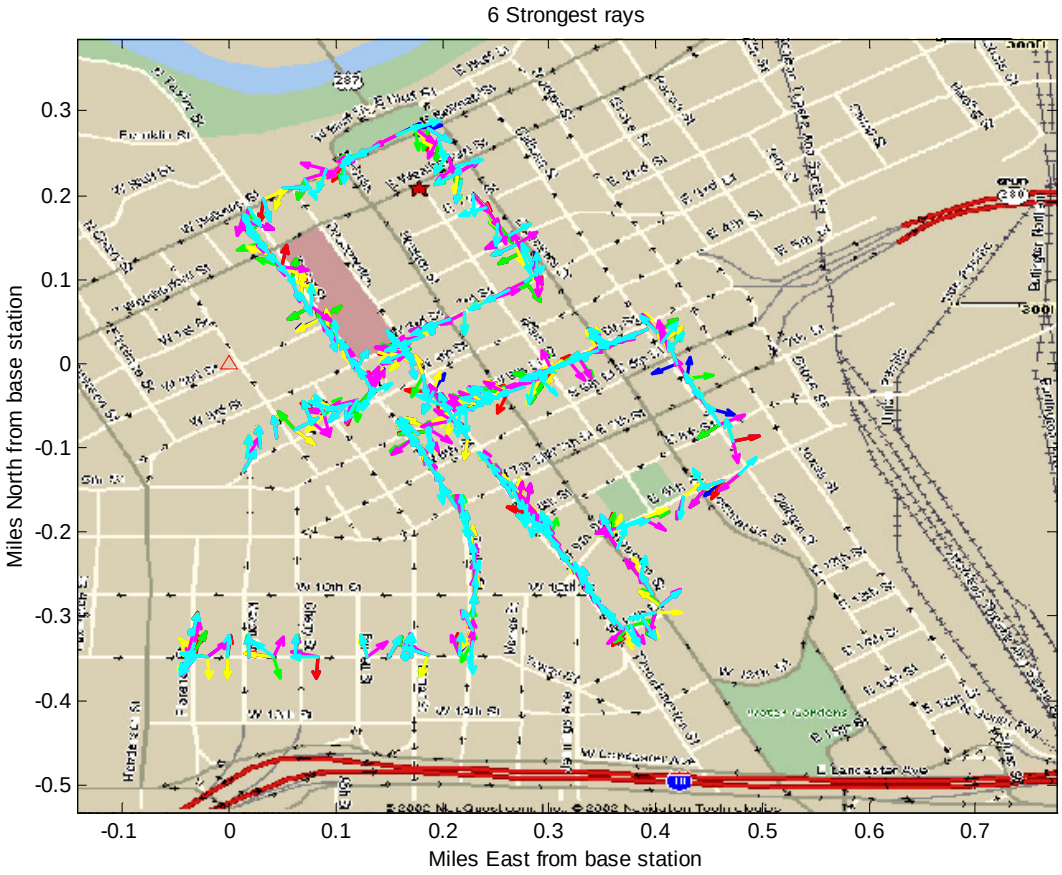

Figure 6 Angle of Arrival versus Path Strength

The arrows in Figure 6 indicate the Angle of Arrival for the strongest path. Significant street channeling is evident, with orthogonal paths seen generally occurring at intersections. Along some streets more randomness in AoA is seen.

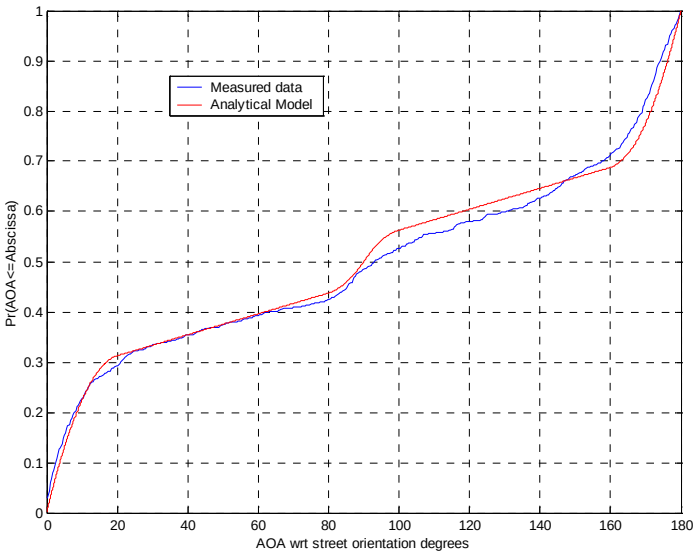

Figure 7 Urban Canyon AoA Probabilities

The statistical results are shown in Figure 7 as a CDF. Notice that there is a high probability, nearly equal to obtain paths from 0^o or 180^o. For these two directions, a range of +/- 20^o contains 60% of the data points. There is also an effect centered around +/-90^o which has another 10% of the occurrences. All paths of various powers were observed to have approximately the same behavior in probability of AoA from this data.

5.1 Proposed Model

An urban canyon model is proposed without the complexities of streets or building grids. The model would simply impose a limited set of angles of arrival for paths received at the UE, referenced to an assumed mobile direction of travel. Thus 0^o shown in Figure 7 would be the reference direction of travel, which assumes that the user or vehicle is moving down the street. An equal probability of seeing negative angles is assumed. Then angles for the 6 paths are chosen from the CDF in Figure 7. There is extremely high correlation between ray AoAs in this model with the strongest paths being 98% correlated.

6. CONCLUSION

In this contribution, a dual-polarization channel model has been presented that is compatible with the current models under discussion. A number of steps are shown to describe the generation procedure.

A randomization method is shown to add realism to the Power Delay Profile. The noise model effects the statistics on a per-drop basis, but does not significantly change the average statistics.

A number of parameter questions about the micro-cell model have been presented. Clarification on these issues will improve our understanding and ability to implement such a model.

A simple Urban Canyon model is proposed that defines AoAs based on a reference orientation. Measured data was shown to illustrate the probability of each AoA. The angles for the 6 paths are chosen from the CDF in Figure 7.

7. APPENDIX A

7.1 Introduction

A dual-polarization channel model is presented based on a simple extension of the single-polarization channel models that are currently being proposed within the 3GPP/3GPP2 Joint Spatial Channel Modeling Ad-hoc discussion [9-11]. This model is based largely on the empirical results reported in the literature which indicate that the mean delay, RMS delay spread, mean azimuth, and azimuth spread is virtually identical for both polarizations [12,13].

7.2 Model Overview

The dual-polarization channel model essentially extends the single-polarization model by allowing each ray to be depolarized by the scattering environment. This is illustrated in Figure 1, where the rays generated in the typical single-polarization scenario are reflected at different polarizations than they were originally transmitted.

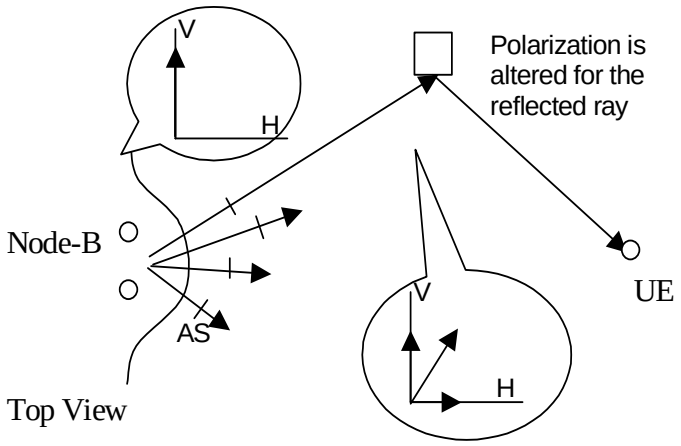

Figure 8 Depolarization Example

In the proposed dual-polarization model, the channel models currently under discussion in the 3GPP/3GPP2 Joint Spatial Channel Modeling Ad-hoc group would be extended as follows:

1. The channel models currently under discussion would be used to generate the channel model for the polarization of the transmitting antenna.
2. A second channel model would then be generated to model the channel corresponding to the polarization orthogonal to the transmitting polarization. This second channel model would have the identical number of rays and sub-rays, identical delays, and identical angles of arrival at the node B and node UE. However, it would have different ray amplitude characteristics which would be set based on a model of the branch power ratio.

7.3 Computation of the Complex Channel Impulse Response

Computation of the channel impulse response between the j^{th} transmit antenna and the k^{th} receive antenna is performed in a manner similar to that used for the single-polarization scenario, with the exception of two important differences. First, the impact of the orthogonal polarization $P_j\perp$ must be included in the calculation in addition to the transmitted polarization P_j. Second, the impact of the different antenna orientations must be included in the computation. This has the effect of producing azimuth-dependent attenuation of the subray amplitudes due to non-vertical orientation.

The process typically used to account for this azimuth dependent attenuation consists of decomposing the transmitted and orthogonal polarizations into vertically-polarized (V) and horizontally-polarized (H) components [14]. As an example, consider the dual-polarized system illustrated in Figure 2. It consists of a node UE array consists of a pair of antenna elements (UE_1 and UE_2) installed in the XY plane slantwise relative to the vertical direction (Y) at angles of α_{T1} and α_{T2} (measured counter-clockwise with w.r.t. the Y-axis), respectively. Similarly, the node B array consists of a pair of antenna elements (BS_1 and BS_2) installed slantwise relative to the vertical direction at angles of α_{R1} and α_{R2}, respectively. Some examples of typical dual-polarized antennas are the slant-45^o configuration (i.e., $\alpha_{T1}=45^o$ and $\alpha_{T2}=-45^o$) and the V-H configuration (i.e., $\alpha_{T1}=90^o$ and $\alpha_{T2}=0^o$).

For subray i that is transmitted from the j^{th} transmit antenna via the transmitting polarization ($h_{jk,i}$), the contribution at the k^{th} receive antenna is computed by first decomposing the sub-ray into its vertical and horizontal components as follows:

$$h_{jk,i,V=} h_{jk,i}\cos(\alpha_{Tj}) \quad (1)$$

and

$$h_{jk,i,H=} h_{jk,i}\sin(\alpha_{Tj}) \quad (2)$$

where the additional subscripts V and H indicate the horizontal and vertical components of the transmitted sub-ray. This is similarly done for the orthogonal polarization ($h_{jk,i\perp}$) as follows:

$$h_{jk,i,\perp,V=} h_{jk,i}\cos(\alpha_{Tj}-\pi/2) \quad (3)$$

and

$$h_{jk,i,\perp,H=} h_{jk,i}\sin(\alpha_{Tj}-\pi/2) \quad (4)$$

where the $\perp$ indicates the contribution of the identical sub-ray in the orthogonal polarization to the transmit polarization. At the kth receive antenna, the contribution of this sub-ray to the composite channel between antennas j and k ($h_{jk,i,total}$) is then added based on its receive orientation, and the impact of the angle of arrivals at the node B and node UE are included. This is performed as follows:

$$h_{jk,i,total} = (h_{jk,i,V}+ h_{jk,i,\perp,V})\cos(\alpha_{Rk})+ (h_{jk,i,H}+h_{jk,i,\perp,V})\sin(\alpha_{Rk})\cos(\beta_{Ti})\cos(\beta_{Ri}). \quad (5)$$

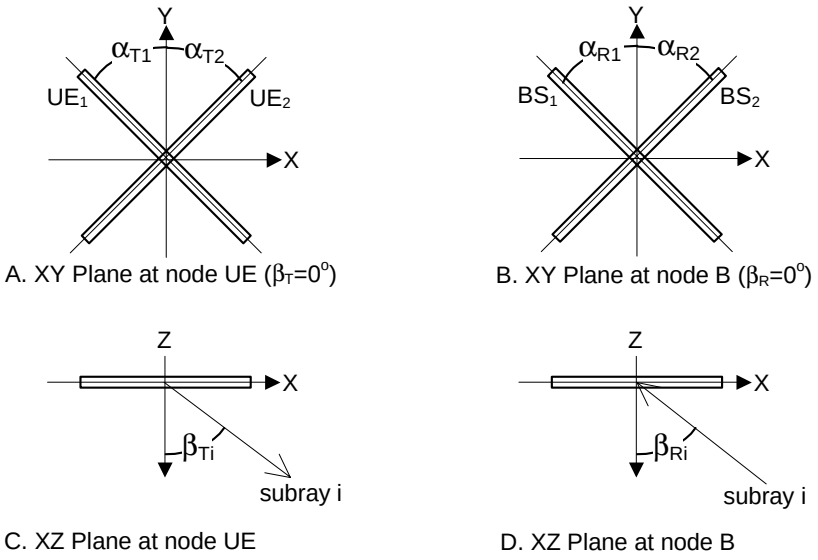

Figure 9 Dual Polarization Example

8. REFERENCES

[1] Motorola, "Model Components and Results for Spatial Channel Model", SCM-048, Seattle WA, USA, August 20-21st 2002.

[2] 3GPP – 3GPP2 SCM AHG Co-Chair, "Spatial Channel Model AHG Ad Hoc Meeting 2 Summary", August 21, 2002.

[3] Lucent, "Updated Wideband System Level Model and Statistics", SCM-045, Seattle WA, USA, August 20-21st 2002.

[4] Motorola, "Mobile Angle Spread Measurements and Angle Distribution Model", TSGR1#24(02)0408, Orlando, Florida, USA, February 18-22, 2002.
[5] Motorola, "Dual Polarization Extension for Spatial Channel Model", SCM-049, Seattle WA, USA, August 20-21st 2002.
[6] 3GPP – 3GPP2 SCM AHG Co-Editors, "Spatial Channel Model Text", SCM-057, September 17, 2002.
[7] Qualcomm, "Standard Deviation of Delays versus RMS Delay Spread", SCM-053, September 17, 2002.
[8] Motorola, "Path Characteristics for Spatial Channel Model", SCM-041, August 1st, 2000.
[9] Motorola, "Correlated Spatial Channel Model", SCM-029, Conference Call, June 4th 2002.
[10] Motorola, "System Level Channel Model and Simulation", TSGR1#24(02)0407, Orlando, Florida, January 18-22, 2002.
[11] Motorola, "Correlated Spatial Channel Model", SCM-020, Conference Call, May 3rd, 2002.
[12] Klaus I. Pedersen, Preben E. Mogensen, and Bernard H. Fleury, "Dual-Polarized Model of Outdoor Propagation Environments for Adaptive Antennas," Vehicular Technology Conference, 1999, pp. 990-995.
[13] P. Eggers, J. Toftgaard, A. Oprea, "Antenna Systems for Base Station Diversity in Urban Small and Micro Cells," IEEE Journal on Selected Areas in Communications, Vol. 11, No. 7, pp. 1046-1057, September 1993.
[14] S. Kozono, T. Tsuruhara, M. Sakamoto, "Base Station Polarization Diversity Reception for Mobile Radio," IEEE Transactions on Vehicular Technology, Vol. VT-33, No. 4, November 1984, pp. 301-306.